

Resonant tunneling in amorphous double-barrier structures

N. Porrás-Montenegro*

Instituto de Física, Universidade Federal Fluminense, 24 020, Niterói, Rio de Janeiro, Brazil

E. V. Anda[†]

Departamento de Física de la Materia Condensada, Universidad Autónoma de Madrid, Madrid 28049, Spain

(Received 30 April 1990)

Using the Kubo formula for the electrical conductivity, and a tight-binding Hamiltonian represented on a Bethe lattice, we have developed a formalism to study the electronic and transport properties of amorphous double-barrier structures. Quantum size effects are analyzed as a function of the parameters of the heterostructure. The theoretical results are compared with I - V experimental curves.

I. INTRODUCTION

Tunneling through heterostructures has received special attention because of its importance due to its practical applications involving negative differential resistance and for the clarification of basic concepts of transport properties in semiconductors.

Since the pioneering work by Tsu and Esaki¹ and by Chang, Esaki, and Tsu² it is well known that resonant tunneling plays a relevant role for perpendicular electronic transport in heterostructures. After the work of Abeles and Tiedje,³ many groups started a new field of research in amorphous semiconductors, such as the study of amorphous semiconductor superlattices free from strict matching requirements, such as, for example, ultrathin multiple-layered structures consisting of amorphous silicon sequentially alternating with other silicon-based material. The unique optical and electrical properties of the multilayer structures have been attributed to the quantized effect in the potential-well layer³⁻⁶ as it manifests itself in crystalline superlattices. Recently several authors have reported resonant tunneling phenomena through amorphous double-barrier structures demonstrating the existence of quantized levels in ultrathin well layers,⁷ as well as the existence of negative differential resistance.⁸

The purpose of this work is to develop a theory to understand simultaneously, and within the context of the same formalism, resonant tunneling and the electronic properties derived from the electronic density of states (DOS) of amorphous semiconductor structures and, in particular, double-barrier devices.

In the past decade there has been a revitalization of band-structure calculations using tight-binding models. They have shown their capability of describing with great accuracy the main features of the electronic bands and the energy of formation of many crystalline, amorphous, and alloy semiconductors using a relatively small local base of five orbitals (sp^3s^*) per site.⁹

The tight-binding representation is particularly suitable for studying the effect of highly correlated local sys-

tems. For semiconductors in particular it is appropriate to study interfaces and disorder because it provides a description in real space where it is natural to represent the breakdown of the translation symmetry.

Formalisms which give a clear and very precise description of the system in the reciprocal space have in general difficulties in treating disorder or systems with interfaces. Some concepts inherent to the existence of the reciprocal space as is, for example, the case of the effective mass, are ambiguous and, rigorously speaking, not valid for these systems.

A significant effort has been made to study the electronic properties of heterostructures and superlattices within the context of the effective-mass approach representing the system by a continuous barrier profile neglecting the existence of a discrete ordered or disordered atomic structure.¹⁰⁻¹² However, for few-layered double-barrier structures for which the de Broglie wave length is comparable to the distance between the atoms or for disordered or amorphous systems with a particular ring statistics they cannot be disregarded at all.

In the present paper we devote our attention to a study of the tunneling in amorphous double-barrier structures (ADBS's) using a tight-binding Hamiltonian which directly takes into account the atoms that constitute the heterostructure including disorder as an essential ingredient. Up to now no theoretical studies have been reported for the density of states and for the electrical conductivity (EC) of ADBS's considering the topology of an amorphous lattice.

The electronic properties derived from an amorphous topology have been extensively studied using the Bethe lattice. Even if it is a simplification of the problem this pseudolattice could be considered as a sort of zeroth-order approximation for the ring statistics of an amorphous lattice because it eliminates all the rings from the structure.¹³ Based on these ideas we represent the amorphous by this pseudolattice.

The transport properties of the system are studied calculating in an exact way the Kubo formula. We believe that the solution of the Kubo formula is the correct way

of studying the nonequilibrium problem relating via linear-response theory the conductance to the equilibrium properties of the system.

Another advantage of the Kubo formalism is that it permits one to obtain the dielectric function of the system and its optical properties as a trivial extension of the frequency-dependent conductivity.

II. THE STRUCTURE SIMULATION BY THE BETHE LATTICE

To study the tunneling in an ADBS we choose a device with structural disorder and simulate it by a Bethe lattice (BL) with the coordination number equal to 4, as is represented in Fig. 1(b). As has already been mentioned,

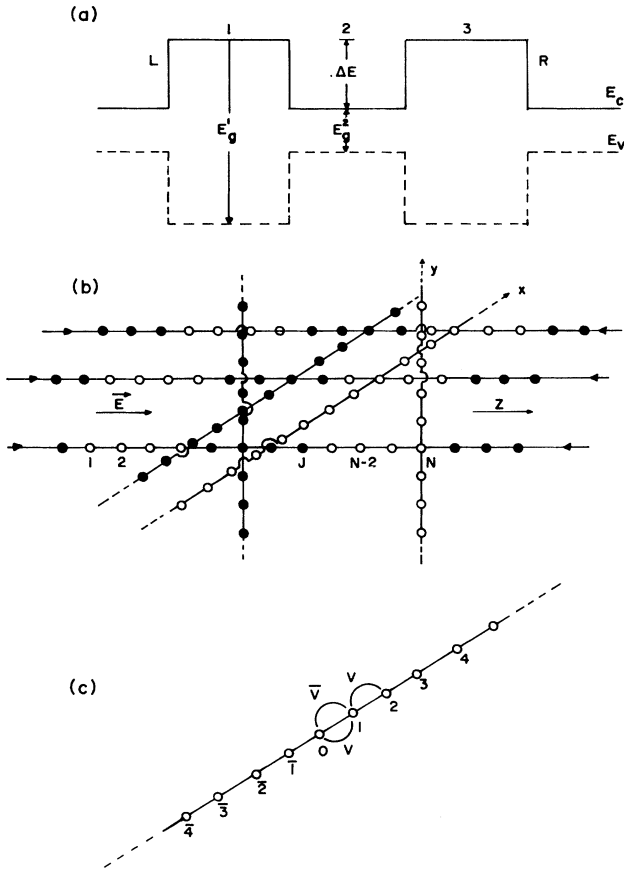


FIG. 1. (a) Schematic energy diagram for a simplified double-barrier single-quantum-well structure. Regions 1 and 3 indicate the barriers and region 2 indicates the well. E_c (E_v) is the conduction- (valence-) band edge of bulk electrodes and quantum-well material. E_g^1 is the bulk energy band gap of the barrier materials 1 and 3 and E_g^2 is the energy band gap of the quantum-well bulk material. (b) Representation of the double-barrier structure in (a) by a Bethe lattice with $Z=4$. The open (solid) circles represent A (B) atoms located at the barriers (well). The dashed arrows represent the semi-infinite Bethe lattice. z is chosen as the resultant transport direction along which the electric field is applied. (c) One of the linear chains perpendicular to the z direction where the decimation procedure is performed.

the BL has been extensively used to study amorphous systems because as it is a ringless pseudolattice it takes into account in a zeroth-order approximation the ring statistics of a structural disorder system. The BL is constructed with a real-space disposition which guarantees that a carrier created at $z = -\infty$ reaches $z = \infty$ going through the double-barrier structure. The open (solid) circles represent A (B) atoms which are located at the barriers (well) and the arrows represent semi-infinite BL. Although it has not been drawn completely, each atom in Fig. 1(b) has four nearest neighbors. Certainly the x and y directions are merely pictorial representations to indicate different linear chains that can be followed in each constituent material of the ADBS. We have supposed the ADBS to be embedded in an infinite amorphous system with a finite and uniform conductivity characterized by an inelastic collision time $\tau = \hbar/\eta$, where η is a parameter which takes into account the scattering due, for example, to the existence of impurities, point defects, and other sources different to the topological amorphicity.

III. HAMILTONIAN, GREEN FUNCTIONS, DENSITY OF STATES, AND CONDUCTIVITY FORMALISM

The heterostructure constituted by N atoms is represented by the nearest-neighbor tight-binding Hamiltonian

$$H = \sum_{i,\sigma} \varepsilon_i n_{i\sigma} + \sum_{i,j,\sigma} V_{ij} c_{i\sigma}^\dagger c_{j\sigma}, \quad (1)$$

where ε_i can assume, in principle, different values depending on its localization i . These different values will permit us to simulate the potential profile corresponding to the heterostructure under the influence of an external electric field. For the case of the double barrier we assume $\varepsilon_i = E_\beta - iev_0/N$ where $E_\beta = E_1$ for adjacent barriers, $E_\beta = E_2$ for the central well, and v_0 is the external potential applied to the system.

For the sake of simplicity the nearest-neighbor hopping matrix elements will be taken constant ($V_{ij} = V$) all along the system. We are representing the Hamiltonian with one orbital per site in which case we restrict ourselves to treat only the valence (conduction) band of the semiconductor.

At zero temperature and for noninteracting electrons the dc EC is obtained by the Kubo formula¹⁴ which in a tight-binding base is given by

$$\sigma(E) = \frac{\theta}{\Omega} \sum_{i,j,k,l} T_{ij} \text{Im}G_{jk}(E+i\eta) T_{kl} \text{Im}G_{li}(E+i\eta) \quad (2a)$$

or

$$\sigma(E) = \frac{\theta}{\Omega} \sum_{i,j} T_{ij} \sigma_{ij}(E) \quad (2b)$$

with

$$\sigma_{ij}(E) = \sum_{k,l} \text{Im}G_{jk}(E+i\eta) T_{kl} \text{Im}G_{li}(E+i\eta), \quad (2c)$$

where G_{jk} is the nondiagonal retarded Green function

and T is the current operator¹⁴ with matrix elements $T_{kl} = V_{kl}(R_k - R_l)$, where R_l corresponds to the spatial coordinate of the atom l . The volume of the system is Ω and $\theta = 2e^2/\pi\hbar$.

It is easy to show that the Green function and the conductivity related quantity

$$P_{ij}^{(\pm)}(E) = \sum_{k,l} G_{ik}(E + i\eta) T_{kl} G_{lj}(E \pm i\eta) \quad (3)$$

satisfy the Dyson matricial equation

$$\underline{Q}^{\pm} = \underline{g}^{\pm} + \underline{g}^{\pm} \underline{X} \underline{Q}^{\pm}, \quad (4a)$$

where the 2×2 matrices \underline{Q}^{\pm} , \underline{X} , and \underline{g}^{\pm} are

$$\underline{Q}_{ij}^{\pm} = \begin{bmatrix} G_{ij}^{\pm} & 0 \\ P_{ij}^{\pm} & G_{ij}^{\pm} \end{bmatrix}; \quad \underline{g}_j^{\pm} = \begin{bmatrix} g_j^{\pm} & 0 \\ 0 & g_j^{\pm} \end{bmatrix} \delta_{ij}; \quad (4b)$$

$$\underline{X}_{ij} = \delta_{i,i+1} \underline{X}^+ + \delta_{i,i-1} \underline{X}^-$$

with

$$\underline{X}^{\pm} = \begin{bmatrix} 1 & 0 \\ \pm 1 & 1 \end{bmatrix}. \quad (4c)$$

The undressed locator g_i^{\pm} is given by

$$g_i^{\pm} = \frac{1}{E \pm i\eta - \varepsilon_i} \quad (4d)$$

and the energy and length are taken in units of V , the nearest-neighbor matrix element, and of a , the lattice parameter.

It is simple to show that the matrix element P_{ij}^{\pm} is related to σ_{ij} of Eq. (2c) through the relation

$$\sigma_{ij}(E) = \frac{1}{2} \text{Re}[P_{ij}^+(E) - P_{ij}^-(E)], \quad (5a)$$

which we call σ_j for a particular point j ,

$$\sigma_j(E) = \frac{1}{2} \text{Re}[P_{j,j+1}^+(E) - P_{j,j+1}^-(E)], \quad (5b)$$

obtaining for the conductivity

$$\sigma(E) = -\frac{\theta}{\Omega} \sum_j \sigma_j(E). \quad (5c)$$

The solution of the Dyson Eq. (4a), and Eq. (5c), gives us simultaneously the DOS and the dc EC of the system for a particular Fermi level $E = E_F$. This formalism to calculate the Kubo formula reduces the problem of calculating the nondiagonal Green function and of summing $Z^2 N^2$ terms (Z is the coordination number) to a problem of calculating the nearest-neighbor nondiagonal matrix elements of the operator P and summing ZN terms given in Eq. (5c).

The Green functions for each site of the linear chain along the z direction in Fig. 1(b) are obtained using the transference matrix method, which allows us to write

$$\underline{Q}_i = [\underline{1} - \underline{g}_i (\underline{X}^- \underline{Q}_{i-1}^L \underline{X}^+ + \underline{X}^+ \underline{Q}_{i+1}^R \underline{X}^-)]^{-1} \underline{g}_i, \quad (6)$$

where

$$\underline{Q}_i^L = (\underline{1} - \underline{g}_i \underline{X}^- \underline{Q}_{i-1}^L \underline{X}^+) \underline{g}_i^{-1} \quad (7)$$

and

$$\underline{Q}_i^R = (\underline{1} - \underline{g}_i \underline{X}^+ \underline{Q}_{i+1}^R \underline{X}^-) \underline{g}_i^{-1}, \quad (8)$$

where we have written for simplicity $\underline{Q}_i = \underline{Q}_{ii}$.

The quantities \underline{Q}_i^L and \underline{Q}_i^R refer to surface Green functions of a semi-infinite structure which begins at $-\infty$ (L) and $+\infty$ (R) and end at site i .

The local density of states (LDOS) at site i is given in terms of the diagonal matrix element of $\underline{Q}_i(E)$, $G_{ii}(E)$ by

$$\rho(E) = -\frac{1}{\pi} \text{Im}[G_{ii}(E)]. \quad (9)$$

The matrix element P_{ij}^{\pm} in Eq. (3) necessary to evaluate the EC is found as follows: The left and right surface Green functions for two adjacent sites of the chain at k and $k+1$ are related through the equation

$$\underline{Q}_{k,k+1} = \underline{Q}_k^L \underline{X}^+ (\underline{Q}_{k+1}^R + \underline{Q}_{k+1}^R \underline{X}^- \underline{Q}_{k,k+1}) \quad (10)$$

from which we obtain

$$P_{k,k+1}^+ = \frac{G_k^L + G_{k+1}^R}{1 - G_k^L + G_{k+1}^R} \quad (11)$$

and

$$P_{k,k+1}^- = -\frac{(p_k^L + G_k^L) G_{k+1}^R + G_k^L (p_{k+1}^R - G_k^L + G_{k+1}^R G_{k+1}^R)}{(1 - G_k^L + G_{k+1}^R)(1 - G_k^L - G_{k+1}^R)}, \quad (12)$$

where the superscripts $+$ and $-$ refer to those of g_i in Eq. (4d) used to calculate the matrix elements of Eq. (4b) and G_k (p_k) corresponds to the diagonal (nondiagonal) matrix element of the surface Green function \underline{Q}_i in Eq. (6).

We solved the BL by decimating¹⁵ linear chains which are, for example, along the x axis as shown in Fig. 1(c). Each atom of this chain has already been renormalized with the information given by Eq. (6) which, as it was analyzed before, corresponds to the chain along the z axis.

According to Fig. 1(c) the decimating equations are

$$\begin{aligned} \underline{G}_{00} &= \underline{g}_0 + \underline{g}_0 \underline{V}_{01} \underline{G}_{10} + \underline{g}_0 \underline{V}_{0\bar{1}} \underline{G}_{\bar{1}0}, \\ \underline{G}_{10} &= \underline{g}_1 \underline{V}_{10} \underline{G}_{00} + \underline{g}_1 \underline{V}_{12} \underline{G}_{20}, \\ \underline{G}_{\bar{1}0} &= \underline{g}_{\bar{1}} \underline{V}_{\bar{1}0} \underline{G}_{00} + \underline{g}_{\bar{1}} \underline{V}_{\bar{1}2} \underline{G}_{\bar{2}0}, \\ \underline{G}_{20} &= \underline{g}_2 \underline{V}_{21} \underline{G}_{10} + \underline{g}_2 \underline{V}_{23} \underline{G}_{30}, \\ \underline{G}_{\bar{2}0} &= \underline{g}_{\bar{2}} \underline{V}_{\bar{2}1} \underline{G}_{\bar{1}0} + \underline{g}_{\bar{2}} \underline{V}_{\bar{2}3} \underline{G}_{\bar{3}0}, \end{aligned} \quad (13)$$

from which we obtain for the undressed renormalized site Green function

$$\underline{g}_0'' = [1 - \underline{g}_0(\bar{V}_{01}\underline{g}_1\underline{V}_{10} + \bar{V}_{0\bar{1}}\underline{g}_{\bar{1}}\underline{V}_{\bar{1}0})]^{-1}\underline{g}_0, \quad (14)$$

where \bar{V}_{01} and \underline{V}_{10} are renormalized according to

$$\bar{V}_{02} = [1 - \underline{g}_0(\bar{V}_{01}\underline{g}_1\underline{V}_{10} + \bar{V}_{0\bar{1}}\underline{g}_{\bar{1}}\underline{V}_{\bar{1}0})]^{-1}\bar{V}_{01}\underline{g}_1\underline{V}_{12} \quad (15)$$

and

$$\underline{V}_{20} = [1 - \underline{g}_2(\underline{V}_{21}\underline{g}_1\underline{V}_{12} + \underline{V}_{29}\underline{g}_9\underline{V}_{92})]^{-1}\underline{V}_{21}\underline{g}_1\underline{V}_{10}, \quad (16)$$

where, initially, \bar{V}_{01} and \underline{V}_{10} are 2×2 identity matrices. Then we dress each point of the chain along z with the renormalized result and repeat the process until convergence. We get through this procedure the matrix elements necessary to obtain the DOS, and the EC using Eqs. (9) and (5b). Although we choose the z direction to use the transference matrix method in our process to solve the BL, we include through the hopping the conductivity contributions between nearest neighbors oriented in other directions when we renormalize linear chains like that in Fig. 1(c). This is equivalent to saying that the topological amorphicity is taken into account in the conductivity calculation through the local density of states.

For the case of linear response the system is in thermodynamical equilibrium and the Fermi level is a clear concept, its value being the same along the structure. However, under the influence of a moderated applied external voltage v_0 , even if the Fermi level is still a useful concept, it has to be considered site dependent. In this case the quantity $\sigma_j(E)$ should be defined with a site-dependent E_F^j , $\sigma_j(E_F^j)$, in which case the conductivity will be a function of the Fermi level of the left source E_{FL} and of the right source E_{FR} such that $ev_0 = E_{FL} - E_{FR}$,

$$\sigma(E_{FL}; v_0) = -\frac{\theta}{\Omega} \sum_j \sigma_j(E_F^j) \text{ for } E_{FL} > E_F^j > E_{FR}, \quad (17)$$

where the variation of the Fermi level with the position j will be assumed to be linear between E_{FL} and E_{FR} ,

$$E_F^j = E_{FL} - ev_0 j / N_z, \quad (18)$$

with N_z the number of atomic layers in the z direction and j the order number of each layer in which we consider constant the Fermi level for a particular value of the external applied voltage. A more sophisticated assumption requires the self-consistent solution of the charge profile in the presence of an electrical current, which is outside the scope of this paper.

To calculate the current of the system by means of the linear-response theory we decompose the applied voltage in infinitesimal contributions. Each of them can be considered as an infinitesimal electric-field perturbation on the system every time it has reached a stationary situation. The contribution to the current which circulates along the structure due to these infinitesimal electric-field perturbations is found integrating them from zero to v_0 . Then

$$I(E_{FL}; v_0) = \int_0^{v_0} \sigma(E_{FL}, v) dv, \quad (19)$$

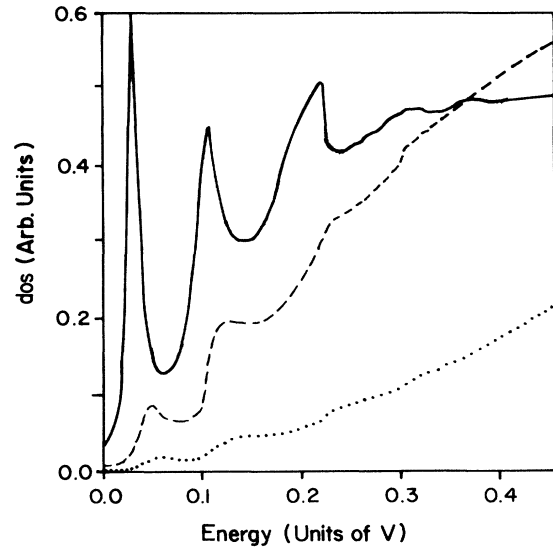


FIG. 2. Local density of states for an ADDBS with $E_1 = 0.5$, 20 layers in the barrier and 30 in the well, at the center (solid curve) and at the border of the well (dashed curve) and at the barrier border (dotted curve).

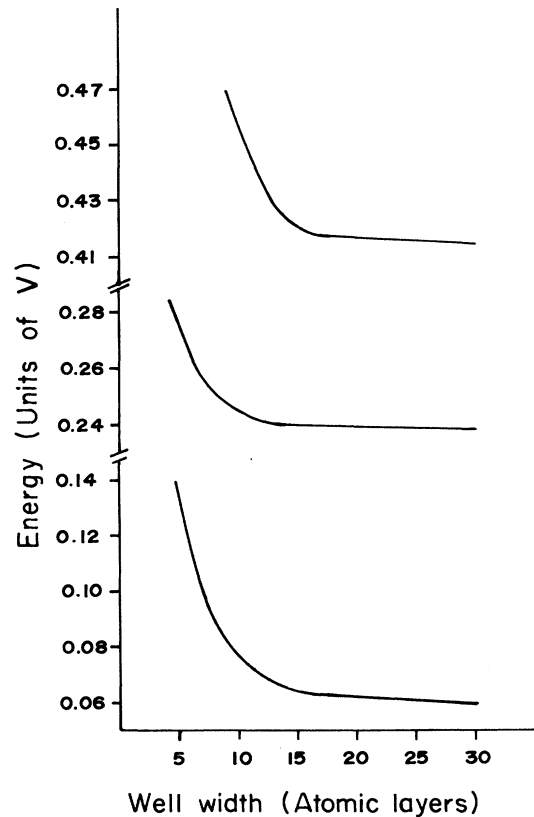


FIG. 3. Variation of the first three resonant energy levels as a function of the well width in an ADDBS with $E_1 = 1.0$, $N_1 = 6$, and $\eta = 0.05$.

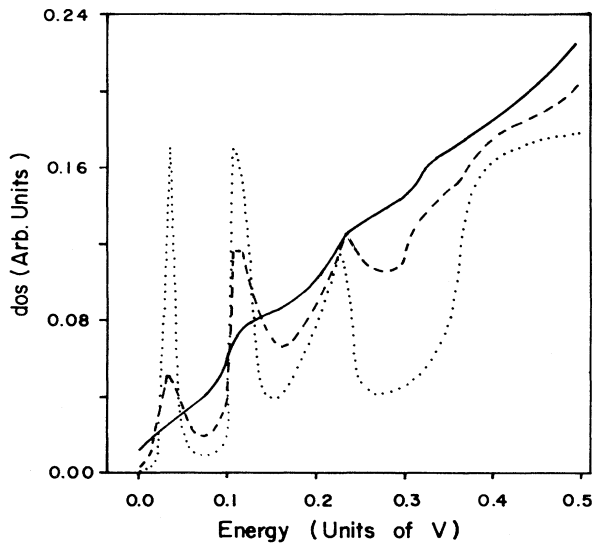


FIG. 4. Local density of states at the center of the well in an ADBS with $E_1=0.5$, $N_1=10$, $N_2=30$, and $\eta=0.05$ (solid curve), $\eta=0.025$ (dashed curve), and $\eta=0.005$ (dotted curve).

where v_0 is the external applied voltage. By virtue of Eq. (18) it is obvious that the Fermi level through the structure will take values accordingly with the infinitesimal decomposition of the applied voltage.

IV. RESULTS AND DISCUSSION

With the formalism developed before we study the ADBS analyzing the LDOS at different atomic positions and the behavior of the total DOS and the EC as a function of E and E_F for different barrier widths and well widths. We study systematically the variation of the resonant level position as a function of the well width and barrier thickness. We also study the I - V characteristics of the device and compare it with recent experimental results.

The number of layers in the barrier N_1 and in the well N_2 determine the width of the device. E_1 is the height of the barrier measured from the bottom of the well in units of V which we take equal to unity.

As an example the local density of states for an amorphous double-barrier structure with $E_1=0.5$, 20 layers in the barrier and 30 in the well are presented in Fig. 2 at the center and the border of the well (solid and dashed curves) and in the first atom inside the barrier after the well border (dotted curve). As expected the resonant levels manifest themselves as sharp peaks in the well, with a smoother behavior at the border and even less structure inside the barrier.

In Fig. 3 we present the variation of the first three resonant level positions as a function of the well width for $E_1=1.0$, $N_1=6$, and $\eta=0.05$. As is observed when the well width is increased, the positions of the resonant levels go to lower values varying strongly for small well widths and slowly for large values of the well width. Also, in our study we found that the position and the

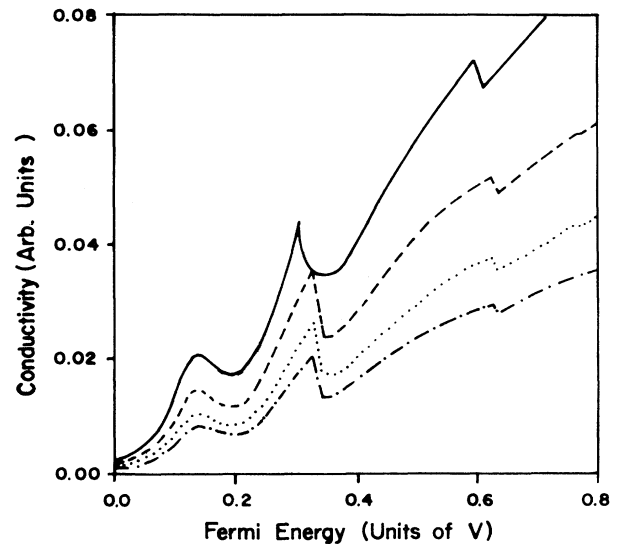


FIG. 5. Conductivity as a function of the Fermi level for an ADBS with $E_1=1.0$, $\eta=0.05$, $N_2=5$, and $N_1=6$ (solid curve), $N_1=10$ (dashed curve), $N_1=15$ (dotted curve), and $N_1=20$ (dot-dashed curve).

number of the resonant peaks are basically independent of the barrier thickness. This means that in an ADBS with a definite barrier height the quantum size effects are determined by the well width.

In Fig. 4 we present the LDOS for an ADBS with $E_1=0.5$, $N_1=10$, $N_2=30$, and $\eta=0.05$ (solid curve), $\eta=0.025$ (dashed curve), and $\eta=0.005$ (dotted curve). As the magnitude of the inelastic width η is decreased the first two peaks increase in height and decrease in width,

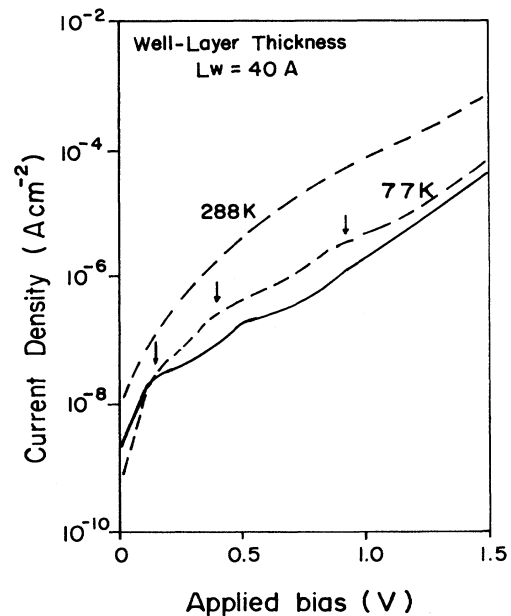


FIG. 6. Experimental I - V characteristics of an ADBS of a - Si_3N_4 : $\text{H}/(p$ -type doped a - $\text{Si:H})/a$ - Si_3N_4 : H in Ref. 7 (dashed curves), and our theoretical result for the same system (solid curve).

indicating that the tunneling is enhanced when the system is free of inelastic scattering.

In Fig. 5 we present the conductivity as a function of the Fermi energy for an ADBS with $E_1 = 1.0$, $\eta = 0.05$, and five layers at the well region with 6 (solid curve), 10 (dashed curve), 15 (dotted curve), and 20 (dot-dashed curve) layers in each barrier. Two effects are observed due to the increase of the barrier thickness: The magnitude of the conductivity is diminished and the position of the higher resonant energy levels is weakly shifted to higher values. This result is in agreement with that found in 1D double-barrier structures.¹⁶

We compare our results with the I - V measurements done on double-barrier structures of a -Si₃N₄:H/ p -type doped a -Si:H/ a -Si₃N₄:H by Miyazaki *et al.*⁷

In Fig. 6 we show the experimental I - V characteristics of Ref. 7 and our results for an ADBS which simulates the experimental device, with a thickness of 46 Å for the barriers, 40 Å for the well, $E_1 = 1.7$ eV, and the effective mass equal to $0.1m_0$ (m_0 being the electron rest mass), which was the better value to make our results coincide with the experiment, instead of the value $0.6m_0$ found by Miyazaki *et al.*⁷ using the electron transmission coefficient treatment, which does not take into account the amorphous and discrete nature of the structure. As mentioned before, the Fermi level is supposed to change through the structure with the same slope as the potential-energy profile, determined by the applied voltage. As observed, we found current bumps similar to those of the experimental situation, but located in slightly different energy position and with some differences in intensity. These bumps in the current correspond to resonant states but are mainly weakened by the topological disorder as our model reflects. From Fig. 1(b) it is clear that our model up to here only simulates ADBS's with one kind of atom in the barrier and another in the well. Obviously in a more realistic situation it is necessary to

consider the contributions due to the thermal smearing of the electron energy distribution and the electron scattering by microscopic fluctuations of the a -Si:H layer thickness as pointed out in Ref. 7, as well as the contribution of the sp^3 orbitals.

V. CONCLUSIONS

We have developed a formalism capable of studying simultaneously the electronic and transport properties of amorphous double-barrier structures using a model Hamiltonian which incorporates the discrete nature of the potential as it is created by the atoms of the semiconductor structure.

Additionally we found that in the ADBS the positions of the resonant energy levels are practically independent of the barrier thickness, which means that the quantum size effects are entirely due to the well width and barrier height. Also we found, as is well known, that reducing the inelastic width η the resonant tunneling is more selected in energy and enhanced but essentially at energies near the barrier height.

The positions of the peaks and the general shape of the experimental I - V curves for ADBS can be well reproduced by our formalism. We believe that the inclusion of p and s^* orbitals in our model, which certainly will complete the description of the system, will permit us to have a better correspondence with the measured results of the relative intensities. Work in this direction is in progress.

ACKNOWLEDGMENTS

One of us (N.P.M.) would like to thank the Brazilian Conselho Nacional de Desenvolvimento Científico e Tecnológico (CNPq) for financial support. This work was partially supported by the Brazilian Agencies CNPq and Finep.

*Permanent address: Departamento de Física, Universidad del Valle, A.A. 25.360, Cali, Colombia.

†Permanent address: Instituto de Física, Universidade Federal Fluminense, Outeiro de São Batista s/n, 24.020 Niterói, Rio de Janeiro, Brazil.

¹R. Tsu and L. Esaki, *Appl. Phys. Lett.* **22**, 562 (1973).

²L. L. Chang, L. Esaki, and R. Tsu, *Appl. Phys. Lett.* **24**, 593 (1974).

³B. Abeles and T. Tiedje, *Phys. Rev. Lett.* **51**, 2003 (1983).

⁴H. Munkata and H. Kukimoto, *Jpn. J. Appl. Phys.* **22**, L544 (1983).

⁵J. Kakaios, H. Fritzsche, N. Ibaraki, and S. R. Ovshinsky, *J. Non-Cryst. Solids* **66**, 339 (1984).

⁶M. Hirose and S. Miyazaki, *J. Non-Cryst. Solids* **66**, 327 (1984).

⁷S. Miyazaki, Y. Ihara, and M. Hirose, *Phys. Rev. Lett.* **59**, 125 (1987).

⁸I. Pereira, M. N. P. Carreno, R. K. Onmori, C. A. Sasaki, A. M. Andrade, and F. Alvarez, *J. Non-Cryst. Solids* **97&98**, 871 (1987).

⁹P. Vogl, H. P. Halmanson, and J. D. Dow, *J. Phys. Chem. Solids* **44**, 365 (1983).

¹⁰J. D. Bruno and T. B. Bahder, *Phys. Rev. B* **39**, 3659 (1989).

¹¹A. D. Stone and P. A. Lee, *Phys. Rev. Lett.* **54**, 1196 (1985)

¹²L. A. Cury and N. Studart, *Superlatt. Microstruct.* **4**, 245 (1988).

¹³F. Vonezawa, M. F. Cohen, and J. Singh, *J. Non-Cryst. Solids* **35&36**, 55 (1980).

¹⁴T. Matsubara and Y. Toyosawa, *Prog. Theor. Phys.* **26**, 739 (1961).

¹⁵J. d'Albuquerque e Castro, *J. Phys. C* **17**, 5945 (1984).

¹⁶N. Porrás-Montenegro, A. Latgé, and E. Anda (unpublished).